International Journal of Dynamics of Fluids.
ISSN 0973-1784 Volume 13, Number 2 (2017), pp. 345-362

http://www.ripublication.com

CFD Analysis of a Cross-flow Heat Exchanger with Different fin thickness

K.Ravikumar[1], Ch.Naga Raju[2], Meera Saheb[3]

[1]Assistant Professor, V.R.Siddhartha Engineering College,.
[2]Professor, V.R.Siddhartha Engineering College.
3. Professor, JNTU Kakinada,

Abstract

Efficiency of heat exchanger and its dimensions are ones of the most important parameters to consider in engineering design. The size of heat exchanger can be more compact by introducing the fins to increase the heat transfer rate between the heat exchanger surface and the surroundings. Different engineering methods are used in heat exchanger design process. The proper correlations or modeling and simulation tools are often applied to receive the general recommendation at early stages of exchanger study. The performance of the fin-tube heat exchanger for different fin thickness is calculated. To give indications about the accuracy of numerical outcome, the most popular correlations are evaluated and results obtained from Ansys CFX program are verified. Analyzing the output, it seems that the implementation of the CFD model offers particular benefits especially when minor modification are applied to the fin surface for which the correlation equations are not defined. The objective of the present work is to simulate the 3D geometry for cross flow smooth and finned tube heat exchanger with using hot water inside the tube and cooling air outside the tube by using computational fluid dynamic (ANSYS-FLUENT 15). The enhancement of heat transfer has been introduced in many fields of industrial and scientific applications. For the simulation, purpose a symmetric view of the simplified geometry of the heat exchanger is made using solid works software.

Keywords: Heat exchanger, Fin thickness, CFX, CFD,

1. Introduction

Heat exchangers are devices used to transfer heat energy from one fluid to another. Typical heat exchangers experienced by us in our daily lives include condensers and evaporators used in air conditioning units and refrigerators. Boilers and condensers in thermal power plants are examples of large industrial heat exchangers. There are heat exchangers in our automobiles in the form of radiators and oil coolers. Heat exchangers are also abundant in chemical and process industries. Different heat exchangers are named according to their applications. For example, heat exchangers being used to condense are known as condensers; similarly heat exchangers for boiling purposes are called boilers. Performance and efficiency of heat exchangers are measured through the amount of heat transferred using least area of heat transfer and pressure drop. A better presentation of its efficiency is done by calculating over all heat transfer coefficient. Pressure drop and area required for a certain amount of heat transfer, provides an insight about the capital cost and power requirements (Running cost) of a heat exchanger. Usually, there is lots of literature and theories to design a heat exchanger according to the requirements. A good design is referred to a heat exchanger with least possible area and pressure drop to fulfill the heat transfer requirements. Cross flow heat exchangers may be finned or corrugated and may be used in single-pass or multipass modes of operation. Flow passages associated with compact heat exchangers are typically small, and the flow is usually laminar.

2. Fin-tube cross-flow heat exchanger geometry

The analysis of heat transfer from finned surfaces involves solving second-order differential equations and is often a subject of researches including also the variable heat transfer coefficient as a function of temperature or the fin geometrical dimensions. In general, the study of the extended surface heat transfer compromises the movement of the heat within the fin by conduction and the process of the heat exchange between the fin and the surroundings by convection [18]. For the ideal case, the optimized profile of the symmetrical radial fin of least material can be found from the generalized differential equation [19]. It leads to the parabolic fin shape for which the heat flux is less sensitive to the variation of the tip temperature than in the case of rectangular and trapezoidal fin profiles. In practice, flow mal distribution is common during the air flow and influences the performance of heat exchangers. The analysis and design of heat exchangers consider problems in which the temperature of the fluid changes as it flows through a passage as a result of heat transfer between the wall and the fluid. For heat transfer analyses, at least the following heat transfer surface geometrical properties are needed on each side of a two-fluid exchanger: minimum free-flow area, core frontal area, heat transfer surface area which includes both primary and fin area, hydraulic diameter, and flow length.

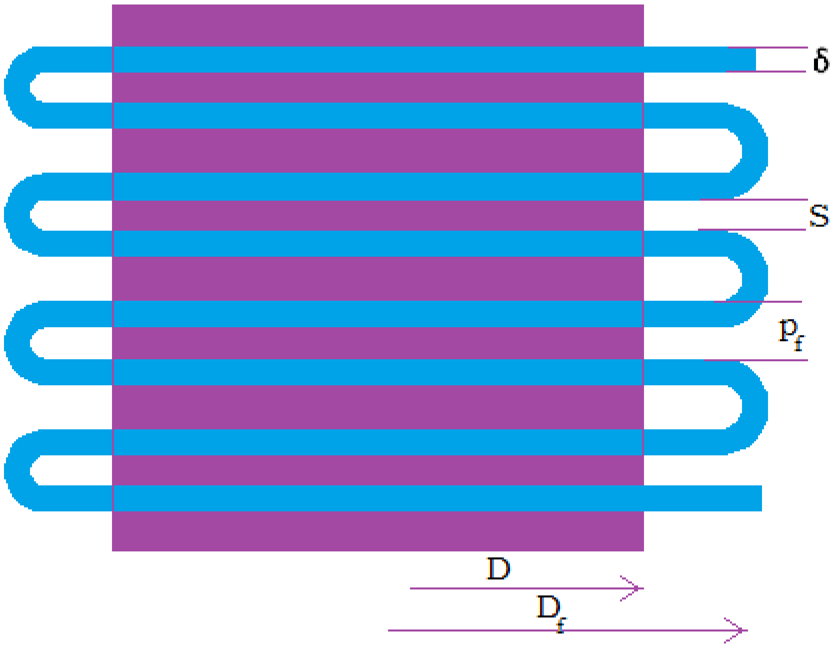

Figure 1: Fin-tube geometry, with minimum cross-sectional area

Surface area of one sector consists of fin and tube are defined as

Surface area of fins: $A_f = \left[\frac{1}{2}\pi\left(D_f^2 - D^2\right)\right] + \pi D_f \delta$

Surface area of tube between fins: $A_t = \pi DS$

Total surface area: $A_T = \pi D\left(S + \delta\right)$

Reynolds number, maximum fluid velocity and Nusselt number is defined as

$$\mathrm{Re}_D = \frac{\rho v_{\max} D}{\eta} \tag{1}$$

$$v_{\max} = \frac{m_f}{A_o \rho} \tag{2}$$

$$\overline{Nu} = \frac{\bar{h} D}{k_f} \tag{3}$$

The heat exchanger characteristic dimensions are written for different fin thickness is tabulated in Table 1:

Table:1: Heat exchanger characteristic dimensions

Fin version	$R_f = D_f / 2$ mm	R=D/2 mm	δ_t mm	P_f mm	P_t mm	δ mm
a	19.5	12.0	2.0	3.0	41	1.0
b	19.5	12.0	2.0	3.0	41	0.9
c	19.5	12.0	2.0	3.0	41	0.7

3.Correlation for external heat transfer in fin-tube cross flow heat exchanger

The value of heat transfer depends on local fluid velocity, fluid properties and details of the tube bank geomentry. Correlations that allow calculating average heat transfer coefficient $\overline{h'}$ are derived from experimental data and take into account geometrical features.

3.1. Recommended correlation to calculate the average Nusselt number for staggered tube banks by Engineering Sciences Data Unit [21]

The correlation can be applied for Reynolds number range $2\times10^3 \le \mathrm{Re} \le 4\times10^4$ and $0.13 < \frac{s}{l} < 0.57$, $1.15 < \frac{X_t}{X_l} < 1.72$:

$$\overline{Nu} = 0.242\,\mathrm{Re}^{0.658} \left(\frac{s}{l}\right)^{0.297} \left(\frac{X_t}{X_l}\right)^{-0.091} .\mathrm{Pr}^{\frac{1}{3}} .F_1.F_2 \quad (4)$$

Where

$X_t = P_t$ -transverse tube pitch

$X_l = longitudinaltubepitch$,

F_1-Factor for fluid property variation

F_2-Factor for number of fin-tube rows (F_2=0.71 is applied for all correlations)

0.98 For four or more rows

0.93 For three rows

0.81 For two rows

0.73 For one row

3.2 Correlation of Briggs and Young [19], [22], [23]

$$\overline{Nu} = 0.134\,\mathrm{Re}^{0.681}\,\mathrm{Pr}^{\frac{1}{3}}.\left(\frac{s}{l}\right)^{0.200}\left(\frac{s}{\delta}\right)^{0.1134} \tag{5}$$

The correlation is based on experimental data for eight row tube banks laid out on equilateral triangular pitch and $1.10^3 \le \mathrm{Re} \le 1.8\times10^4$,11.02<D<40.32mm,1.38<l<16.43mm,0.33mm<δ<1.96mm,0.76mm<s<2.72mm,24.21mm<X_t<109.02mm,

3.3 Effective heat transfer coefficient

Effective heat transfer coefficient , for the air flowing outside and at right angles to the axis of a bank of finned pipes ,can be represented approximately by the dimensional equation[24]:

$$\overline{h'} = \overline{h}\frac{A_f - A_t}{A_T} \tag{6}$$

$$\overline{h} = 5.29\frac{{v_{IN}}^{0.6}}{D^{0.4}}\left(\frac{X_t}{X_t - D}\right)0.6 \tag{7}$$

4. Mean temperature Coefficient and heat transfer in heat exchanger

Total heat transfer can be calculated taking into consideration fin efficiency:

$$Q = \overline{h}\Delta T\left(\eta_f A_f + A_t\right) = \overline{h'}\Delta TA \tag{8}$$

Where

η_f -fin efficiency

$\overline{h'}$ -effective heat transfer coefficient

To evaluate the heat transfer, it is necessary to find the effective mean temperature difference, ΔT. since the fluid temperature changes in fluid flow through the tube bank, the fluid temperature difference ΔT_{Fluid} can be calculated from energy exchanged as:

$$Q = \overline{h}\Delta T\left(\eta_f A_f + A_t\right) = m_f c_f \Delta T_{Fluid} \tag{9}$$

Where

$$\Delta T = \frac{\left(T_0 - T_{OUT}\right) - \left(T_0 - T_{IN}\right)}{\ln \frac{T_0 - T_{OUT}}{T_0 - T_{IN}}} \quad (10)$$

And for

$T_{IN} > T_{OUT}$

$$\Delta T_{Fluid} = T_{IN} - T_{OUT} \quad (11)$$

After transformation

$$\Delta T_{Fluid} = \frac{\bar{h}\left(\eta_f A_f + A_t\right)}{m_f c_f} \Delta T \quad (12)$$

$$T_{OUT} = T_{IN} - \frac{\bar{h}\left(\eta_f A_f + A_t\right)}{m_f c_f} \Delta T \quad (13)$$

$$\Delta T = \left(T_{IN} - T_0\right) \frac{1 - \exp\left[-\frac{\bar{h}\left(\eta_f A_f + A_t\right)}{m_f c_f}\right]}{\frac{\bar{h}}{m_f c_f}\left(\eta_f A_f + A_t\right)} \quad (14)$$

Having calculated effective mean temperature difference, ΔT, average heat transfer coefficient, $\bar{h}$, and fin efficiency, η_f, the rate of heat transfer can be found from Eq.(11)

The fin efficiency value η_f can be achieved from Equation [20]

$$\eta_f = \frac{\tanh\left(\sqrt{\frac{2\bar{h}}{\left(\delta k_f\right)}}.\psi\right)}{\sqrt{\frac{2\bar{h}}{\left(\delta k_f\right)}}.\psi} \quad (15)$$

Where

$$\psi = \frac{D}{2}\left(\frac{D_f}{D} - 1\right)\left(1 + 0.35 \ln \frac{D_f}{D}\right) \quad (16)$$

4. Results of heat transfer calculations

Calculations are done for circular fin-tube heat exchanger. Three-dimensional models are performed to find heat transfer characteristics between a finned tube and the air for different fin shapes in order to find the heat transfer rate between the air and the fin material during the air flow in the cross flow heat exchanger. The model allows considering the heat transfer in three directions. The output is compared with the results received from the correlation formula.

Using the described correlation, the heat transfer is determined based on defined the mass flow rate (inlet velocity 4.0 m/s), inlet temperature of the fluid (300^{o}C) and the internal tube surface temperature (70^{o}C). Values of V_{max}, Nu for one row, effective heat transfer coefficient and fluid outlet temperature, received from correlation functions for each fin version, are written in Table 2.

Table2. Heat exchanger surface and flow parameters for fin version (a), (b) and (c).

	Correlation Eq.(4)			Correlation Eq.(5)			Correlation Eq.(7)		
	(a)	(b)	(c)	(a)	(b)	(c)	(a)	(b)	(c)
V_max	12.30	11.25	10.68	12.30	11.25	10.68	12.30	11.25	10.68
$\overline{Nu}$(one row)	70.19	69.74	68.35	59.86	59.68	60.21	----	----	----
$\bar{h}$w/(m^{2}K)	72.17	71.42	70.34	62.45	62.78	63.76	63.56	63.56	63.56
$T_{OUT, ^oC}$	251.2	247.6	248.4	258.9	258.9	258.9	258.6	259.2	259.2

Numerical analysis is also carried out to examine modified finned tube heat exchangers and the influence of the fin thickness on the heat transfer. The numerical outcome of heat transfer coefficient form 3D model is compared to the results received from the correlations for the fin-tube heat exchanger of uniform fin thickness. Correlations are used to check the numerical calculation of the heat transfer and its accuracy in relation to fin shape modifications.

Results are presented in Table 3, where

$$\Delta = \frac{\Delta T\ \_correlat - \Delta T\ \_\mathrm{correlat}}{\Delta T\ \_correlat} .100\% \tag{17}$$

Table 3. Comparison between numerical calculations and correlations for fin version (a),(b) and (c)

	Correlation Eq. (4)			Correlation Eq. (5)			Correlation Eq. (7)		
	(a)	(b)	(c)	(a)	(b)	(c)	(a)	(b)	(c)
ΔT_Correlat°C	43.1	42.8	42.8	38.4	38.3	38.7	39.8	39.6	38.3
ΔT_model°C	43.6	42.1	41.3	44.2	42.5	40.7	44.3	42.6	40.8
Δ	-1.1 %	1.66 %	3.63 %	-13.12 %	-9.88 %	-4.91 %	-10.15 %	-7.04 %	-6.12 %

4.1 Mesh Generation

Mesh generation is very important step of pre-processing stage because it fits the limits of computational domain. Many engineering applications need mesh generation that is appropriate for the solving of 3D Navier-Stokes equations. In the present work, tetrahedron element is used for 3D geometry mesh. Good mesh is recognized from its generated cells number. For a complex geometry, increase the cells number will increase the resolution and the accuracy, but also this increase will be opposed by increase in computer memory, need for high processor and take more time to complete the solution. At last there must be an optimization between the number of cells generated and the time consumed for the solution process. For the present work, the mesh generation is shown in Figure 2.

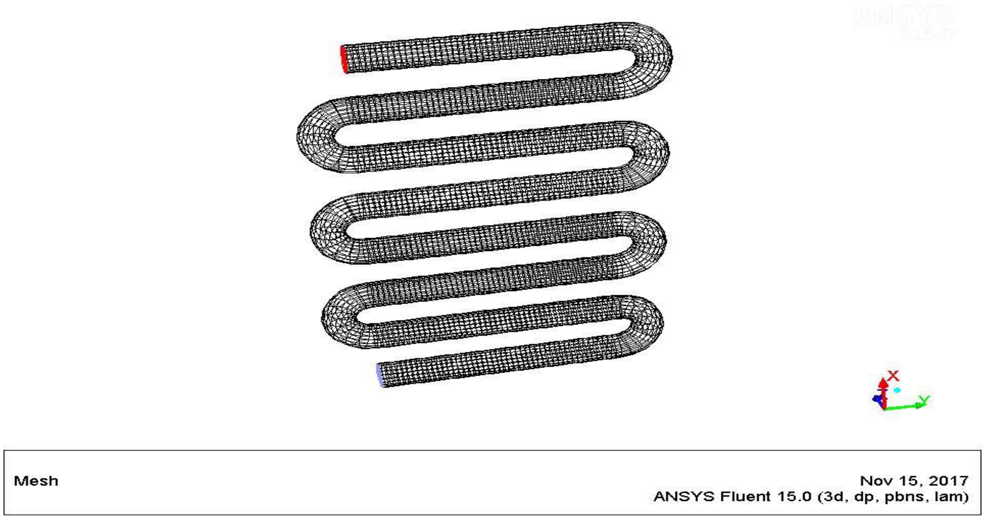

Figure 2: Mesh generation of the present work geometry

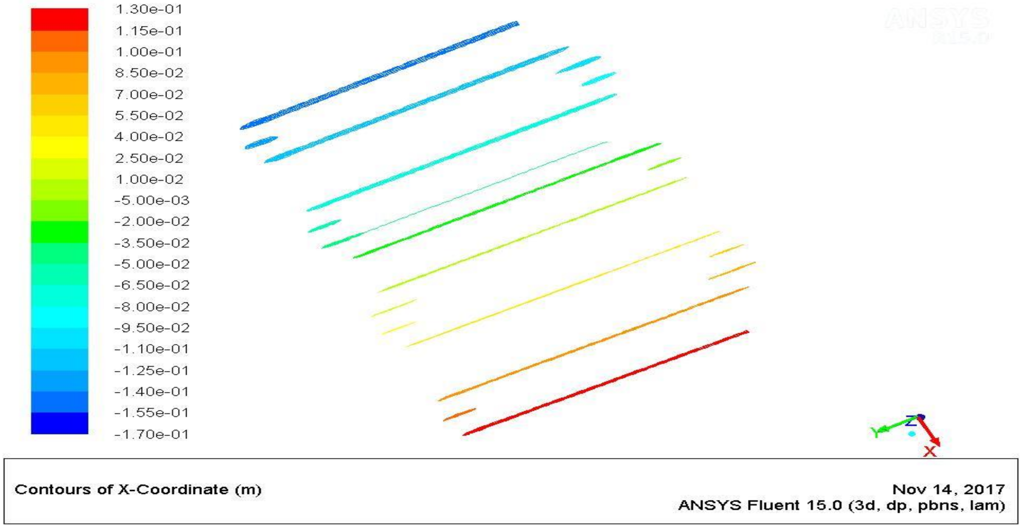

4.2 GOVERNING EQUATIONS

The fundamental basis of most of CFD problems are the solutions of (mass, momentum and energy) equations, as well as the transport equation for turbulent viscosity and its scale. These are in steady state and have been stated below in simple form. For turbulent flow[4]:

5. THE BOUNDARY CONDITIONS

A. Inlet Boundary Conditions

The velocity of the inlet air is limited with a values of (1, 2, 3, and 4) m/s, while the volume flow rate of tube side liquid is limited with a values of (2, 3, 4, 5 and 6) L/min and the temperature of inlet air is the room temperature, while the temperature of tube side liquid is limited with a values of (50, 60, 70 and 80) °C.

B. Outlet Boundary Conditions

The outlet for air side and tube side fluid is specified as pressure outlet and it's represented by the atmospheric pressure.

6 . RESULTS AND DISCUSIONS

The numerical simulation is done by ANSYS FLUENT 15. software to show both the flow field and heat transfer of the present models. Many cases are studied. Three cases are discussed in the following sections. Same boundary conditions are used in the three cases, which are (air velocity of 1 m/s, water inlet temperature and flow rate of (80 °C) and (2 L/min) respectively).

A. Temperature Contours

Figure 3 shows a 3D simulation of temperature distribution in the test section, figures 4. and 5. reveal temperature contours of smooth tube with water and integral finned tube with water. From these figures, it is noted that there is a gradient of temperature distribution along with test tube and the temperature difference are clearly appear in all cases. Also, it is clear from the figures that the temperature gradient of finned tube is higher than that of smooth tube. This means that fining have a substantial effect on increasing the temperature difference inside the test tube.

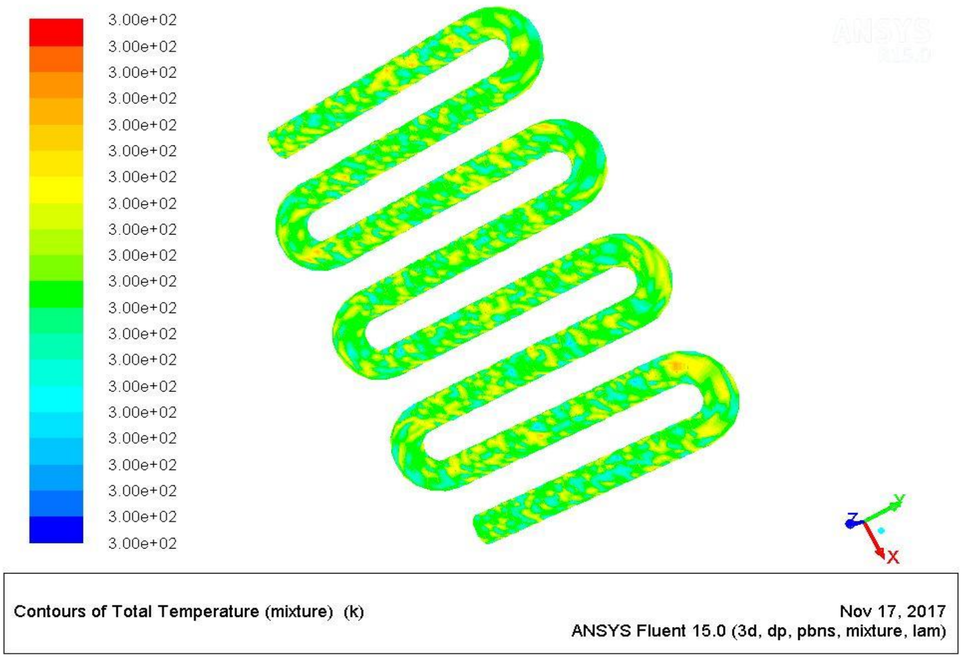

Figure 3(a): shows contours of Total Temperature (mixture) (K)

B. Velocity and Vectors Contours

Figure 4. “(a)” shows a longitudinal section of velocity contour, from figure, the velocity of water inside the tube is constant due to stability of water flow rate. Figure 4. “(b)”demonstrate a cross section of velocity contour, this figure represent the behavior of air through the test section, before the test tube the velocity of air are constant, the air velocity are increased during it across through the passes of test tube, ddies are formed behind the test tube and turbulence is increased.

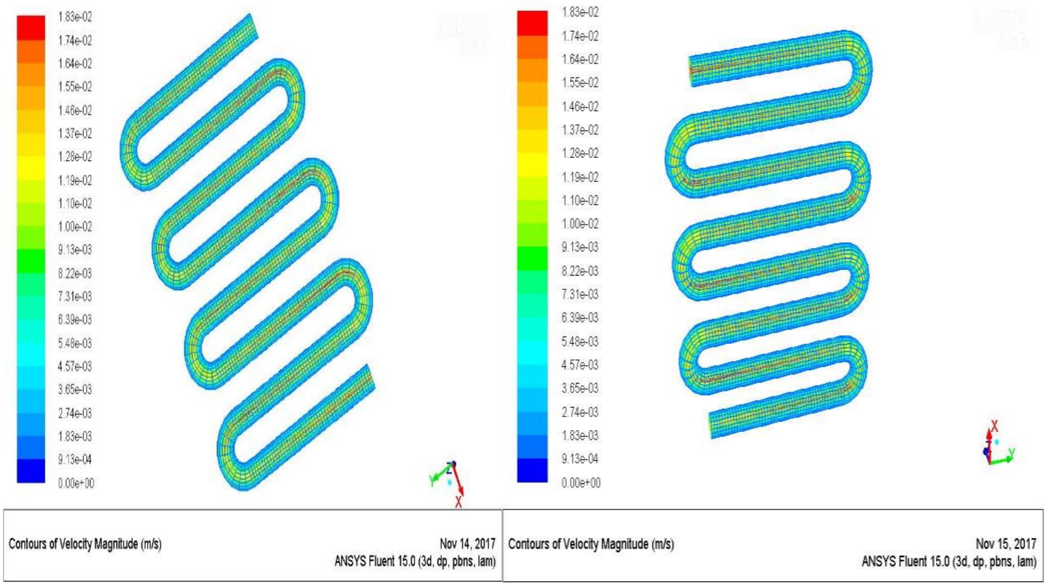

Figure 4 (a) longitudinal section of velocity contour **Figure 4 (b)** cross section of velocity contour

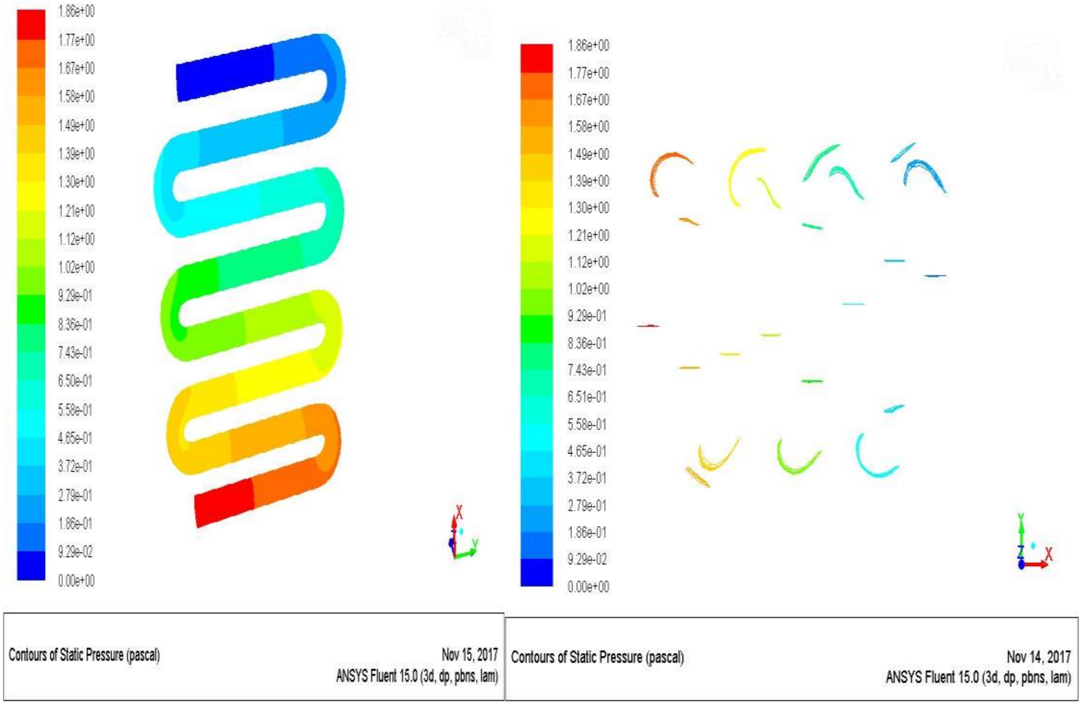

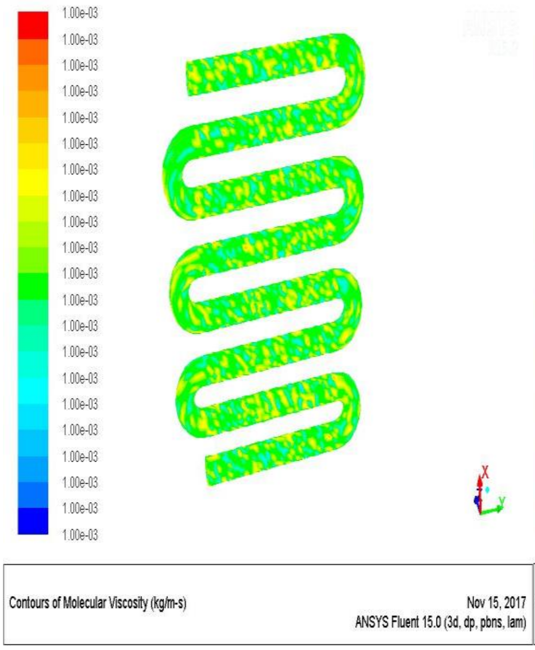
1.00e-03
1.00e-03
1.00e-03
1.00e-03
1.00e-03
1.00e-03
1.00e-03
1.00e-03
1.00e-03
1.00e-03
1.00e-03
1.00e-03
1.00e-03
1.00e-03
1.00e-03
1.00e-03
1.00e-03
1.00e-03
1.00e-03
1.00e-03
1.00e-03
Contours of Molecular Viscosity (kg/m-s)
Nov 15, 2017
ANSYS Fluent 15.0 (3d, dp, pbns, lam)

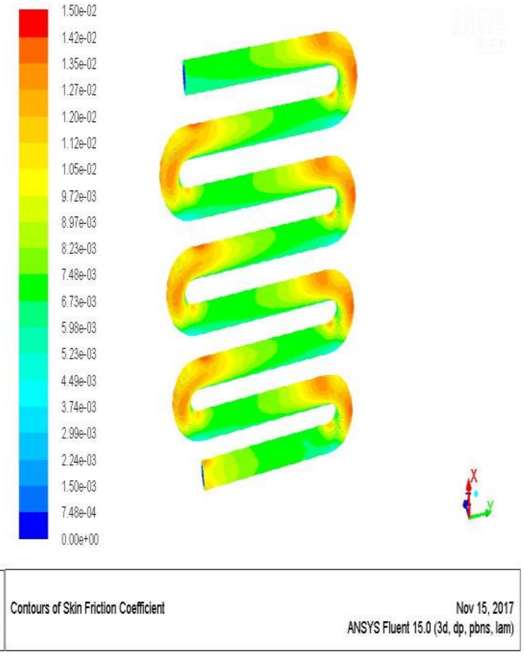
1.50e-02
1.42e-02
1.35e-02
1.27e-02
1.20e-02
1.12e-02
1.05e-02
9.72e-03
8.97e-03
8.23e-03
7.48e-03
6.73e-03
5.98e-03
5.23e-03
4.49e-03
3.74e-03
2.99e-03
2.24e-03
1.50e-03
7.48e-04
0.00e+00
Contours of Skin Friction Coefficient
Nov 15, 2017
ANSYS Fluent 15.0 (3d, dp, pbns, lam)

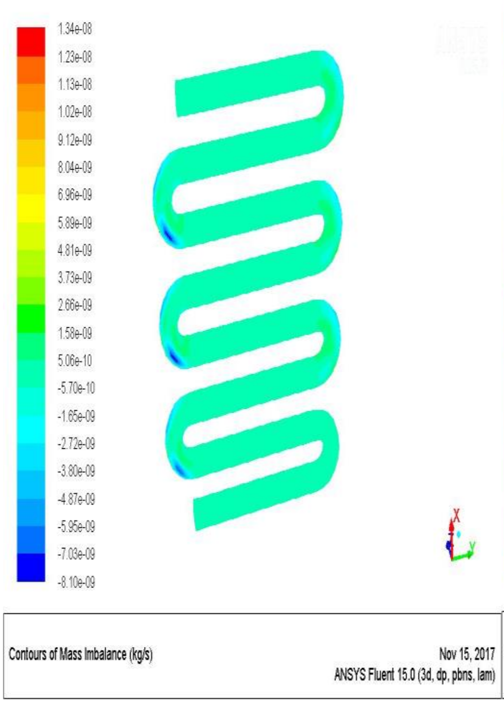
1.34e-08
1.23e-08
1.13e-08
1.02e-08
9.12e-09
8.04e-09
6.96e-09
5.89e-09
4.81e-09
3.73e-09
2.66e-09
1.58e-09
5.06e-10
-5.70e-10
-1.65e-09
-2.72e-09
-3.80e-09
-4.87e-09
-5.95e-09
-7.03e-09
-8.10e-09
Contours of Mass Imbalance (kg/s)
Nov 15, 2017
ANSYS Fluent 15.0 (3d, dp, pbns, lam)

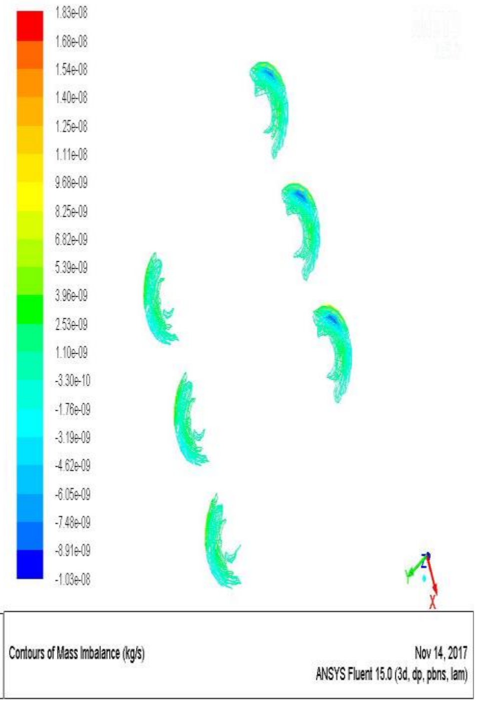
1.83e-08
1.68e-08
1.54e-08
1.40e-08
1.25e-08
1.11e-08
9.68e-09
8.25e-09
6.82e-09
5.39e-09
3.96e-09
2.53e-09
1.10e-09
-3.30e-10
-1.76e-09
-3.19e-09
-4.62e-09
-6.05e-09
-7.48e-09
-8.91e-09
-1.03e-08
Contours of Mass Imbalance (kg/s)
Nov 14, 2017
ANSYS Fluent 15.0 (3d, dp, pbns, lam)

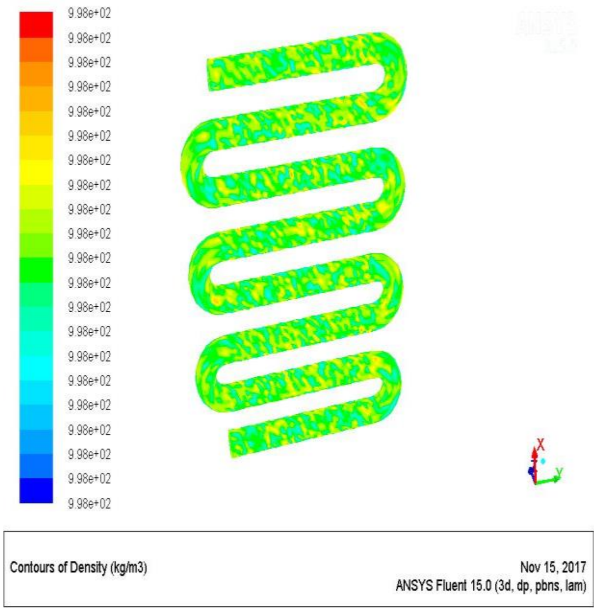
9.98e+02
X
Y
Contours of Density (kg/m3)
Nov 15, 2017
ANSYS Fluent 15.0 (3d, dp, pbns, lam)

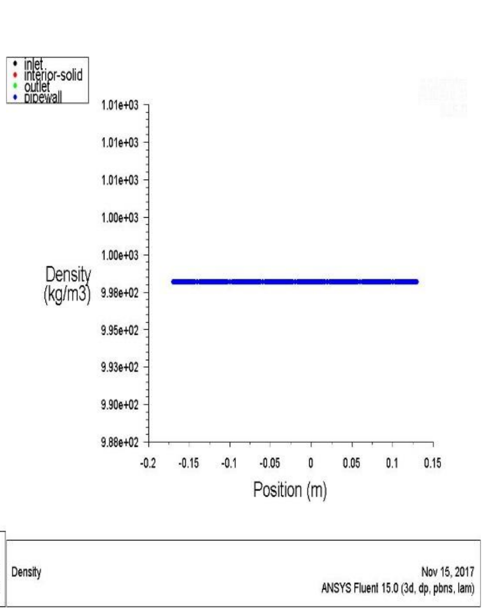
inlet
interior-solid
outlet
pipewall
1.01e+03
1.01e+03
1.01e+03
1.00e+03
1.00e+03
9.98e+02
9.95e+02
9.93e+02
9.90e+02
9.88e+02
Density (kg/m3)
-0.2
-0.15
-0.1
-0.05
0
0.05
0.1
0.15
Position (m)
Density
Nov 15, 2017
ANSYS Fluent 15.0 (3d, dp, pbns, lam)

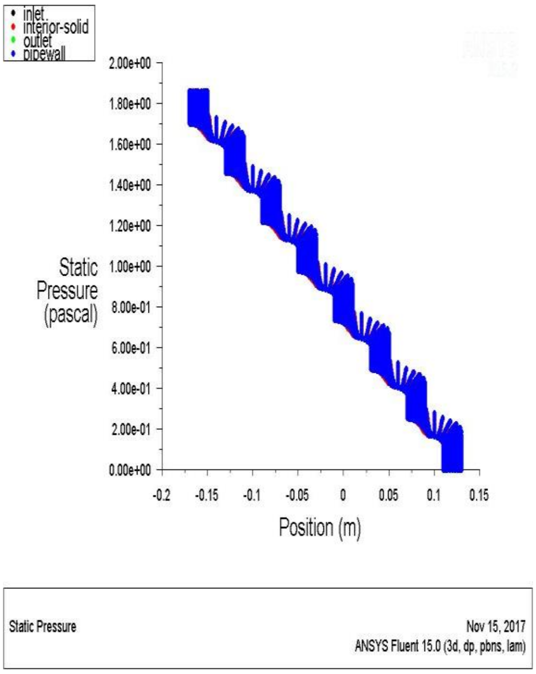
inlet
interior-solid
outlet
pipewall
2.00e+00
1.80e+00
1.60e+00
1.40e+00
1.20e+00
1.00e+00
8.00e-01
6.00e-01
4.00e-01
2.00e-01
0.00e+00
Static Pressure (pascal)
-0.2
-0.15
-0.1
-0.05
0
0.05
0.1
0.15
Position (m)
Static Pressure
Nov 15, 2017
ANSYS Fluent 15.0 (3d, dp, pbns, lam)

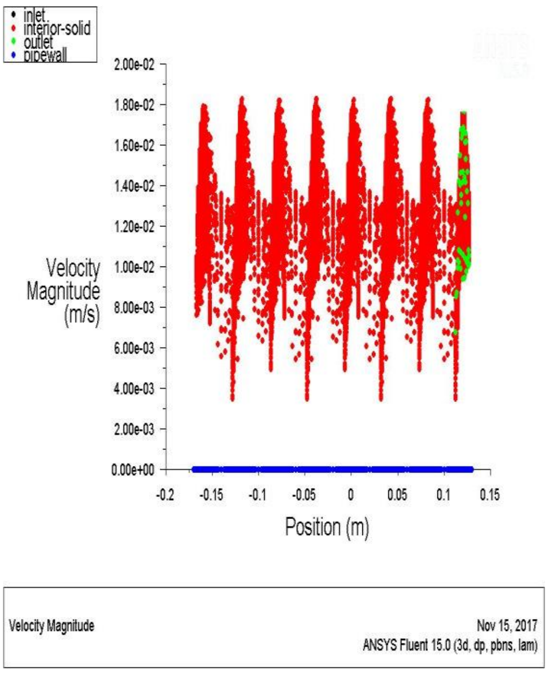
inlet
interior-solid
outlet
pipewall
2.00e-02
1.80e-02
1.60e-02
1.40e-02
1.20e-02
1.00e-02
8.00e-03
6.00e-03
4.00e-03
2.00e-03
0.00e+00
Velocity Magnitude (m/s)
-0.2
-0.15
-0.1
-0.05
0
0.05
0.1
0.15
Position (m)
Velocity Magnitude
Nov 15, 2017
ANSYS Fluent 15.0 (3d, dp, pbns, lam)

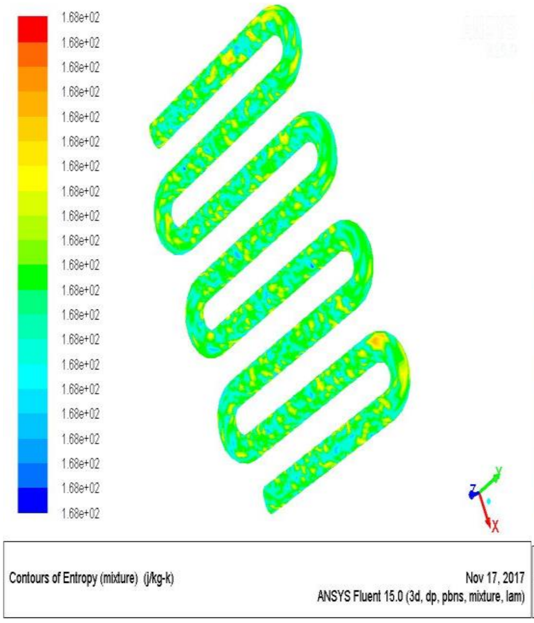
Contours of Entropy (mixture) (j/kg-k)
Nov 17, 2017
ANSYS Fluent 15.0 (3d, dp, pbns, mixture, lam)

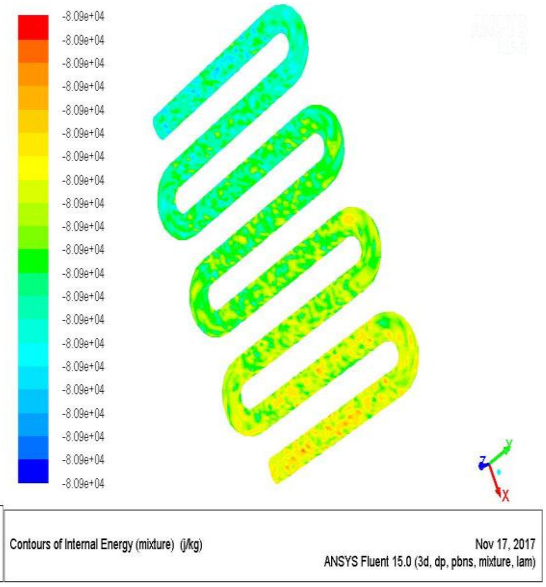
Contours of Internal Energy (mixture) (j/kg)
Nov 17, 2017
ANSYS Fluent 15.0 (3d, dp, pbns, mixture, lam)

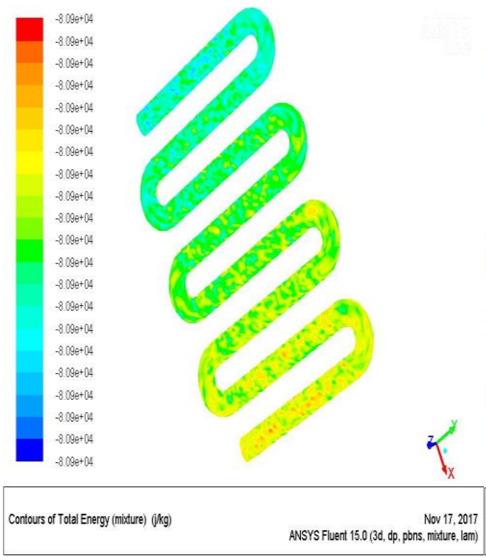
Contours of Total Energy (mixture) (j/kg)
Nov 17, 2017
ANSYS Fluent 15.0 (3d, dp, pbns, mixture, lam)

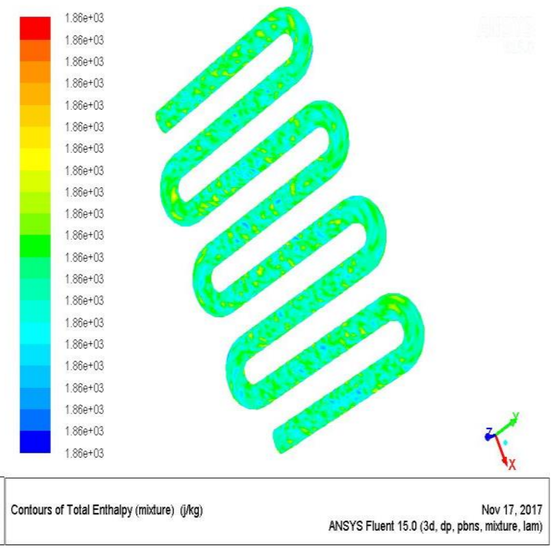
Contours of Total Enthalpy (mixture) (j/kg)
Nov 17, 2017
ANSYS Fluent 15.0 (3d, dp, pbns, mixture, lam)

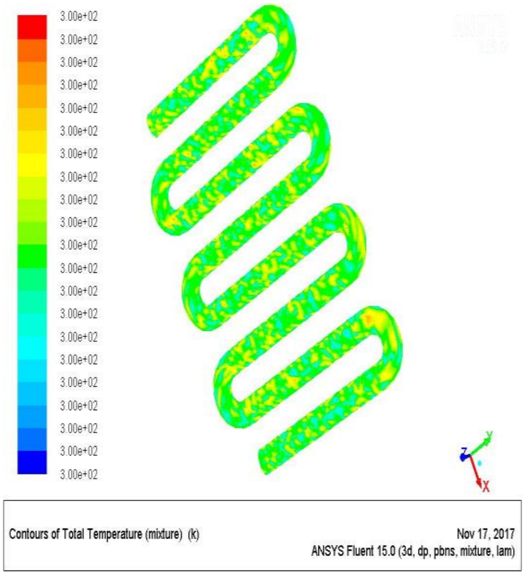
3.00e+02
Contours of Total Temperature (mixture) (k)
Nov 17, 2017
ANSYS Fluent 15.0 (3d, dp, pbns, mixture, lam)

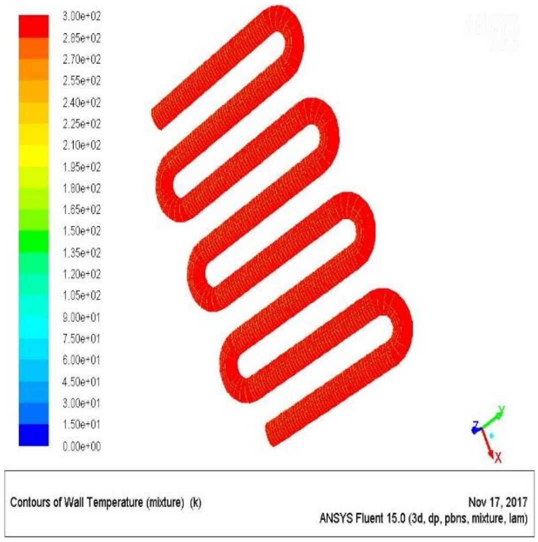
3.00e+02
2.85e+02
2.70e+02
2.55e+02
2.40e+02
2.25e+02
2.10e+02
1.95e+02
1.80e+02
1.65e+02
1.50e+02
1.35e+02
1.20e+02
1.05e+02
9.00e+01
7.50e+01
6.00e+01
4.50e+01
3.00e+01
1.50e+01
0.00e+00
Contours of Wall Temperature (mixture) (k)
Nov 17, 2017
ANSYS Fluent 15.0 (3d, dp, pbns, mixture, lam)

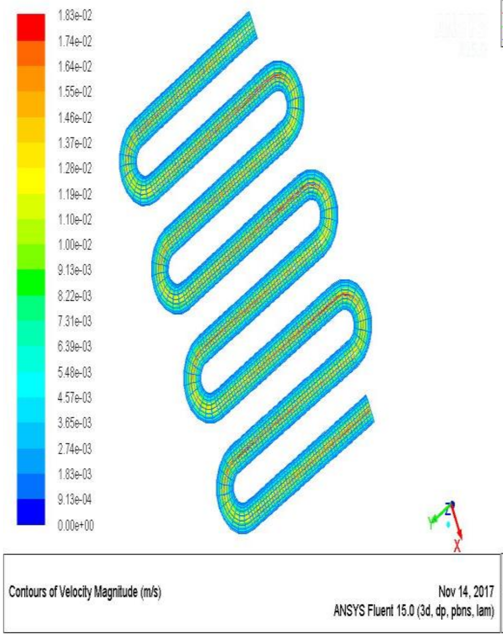
1.83e-02
1.74e-02
1.64e-02
1.55e-02
1.46e-02
1.37e-02
1.28e-02
1.19e-02
1.10e-02
1.00e-02
9.13e-03
8.22e-03
7.31e-03
6.39e-03
5.48e-03
4.57e-03
3.65e-03
2.74e-03
1.83e-03
9.13e-04
0.00e+00
Contours of Velocity Magnitude (m/s)
Nov 14, 2017
ANSYS Fluent 15.0 (3d, dp, pbns, lam)

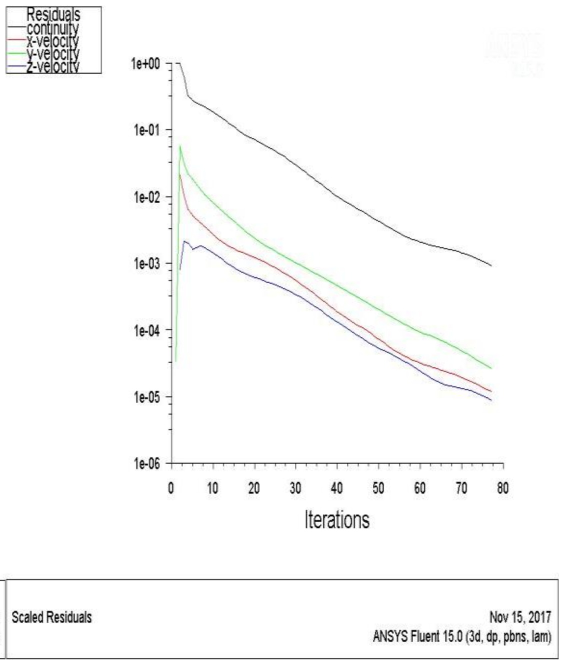
Residuals
continuity
x-velocity
y-velocity
z-velocity
1e+00
1e-01
1e-02
1e-03
1e-04
1e-05
1e-06
0
10
20
30
40
50
60
70
80
Iterations
Scaled Residuals
Nov 15, 2017
ANSYS Fluent 15.0 (3d, dp, pbns, lam)

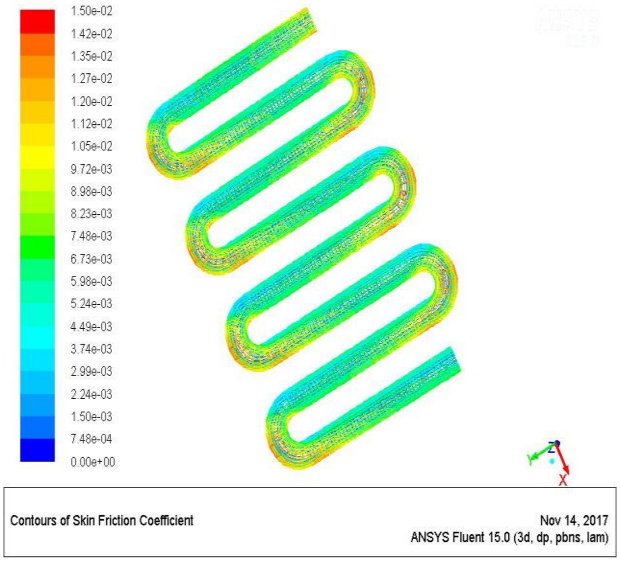

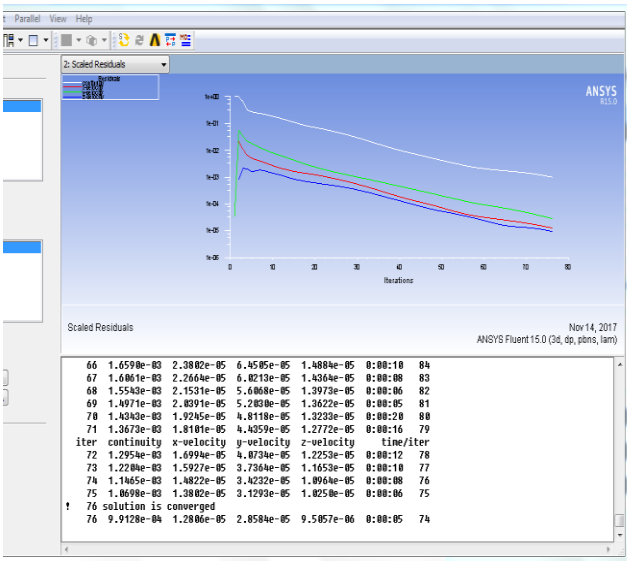

7. CONCLUSIONS

The main objective of this research is to determine numerically the performance of the heat transfer process in a single row fin-tube cross flow heat exchanger for different fin configurations. The most popular correlations are applied for heat transfer evaluation. For Briggs and Young correlation, the heat transfer decreases with the fin thickness increase. The opposite results are seen for the other correlations. The heat transfer is also analyzed by means of numerical computation. The results are verified with the known correlations for circular fins of constant thickness. Analyzing the output received from numerical calculations with those gathered from correlations, it seems that the differences are within the standard deviation and numerical techniques can predict heat transfer coefficients with acceptable accuracy. The use of the CFD model offers particular benefits especially when minor modification are applied to the fin surface for which the correlation equations are not defined, for instance fin thickness modification. However, comparative analyses are still required and the numerical model should be examined, verified with proper correlations or experimental values.

References

[1] P. Wais, One row fin heat exchanger numerical optimization, Proceedings of International Congress on Thermodynamics, 4-7 Sept Poznan, (2011) 709-716.

[2] R. K. Shah, D. P. Sekulic, Fundamentals of Heat Exchanger Design, Wiley, 2003.

[3] P. Wais, Extended Surfaces (Fins and Pins), in: R.B. Hetnarski, Encyclopedia of Thermal Stresses, Vol 3, Springer, Dordrecht, 2014, 1536- 1550.

[4] J. Y. Jang, M. C Wu., W. J. Chan, Numerical and experimental studies of three dimensional plate-fin and tube heat exchangers. International Journal of Heat and Mass Transfer 14 (1996) 3057-3066.

[5] P. Wais, J. Taler, Fin shape optimization in tube heat exchangers by means of CFD program, 2nd International Conference on Engineering Optimization, Sept. 6 - 9, Lisbon, Portugal, (2010) 1-10.

[6] P. Wais, Fluid flow consideration in fin-tube heat exchanger optimization, Archives of Thermodynamics, 31, (2010) 87-104.

[7] W. M. Yan, P. J. Sheen, Heat transfer and friction characteristics of fin-and-tube heat exchangers, International Journal of Heat and Mass Transfer 43, (2000) 1651-1659.

[8] M. S. Mon, U. Gross, Numerical study of fin-spacing effects in annular-finned tube heat exchangers. International Journal of Heat and Mass Transfer 47, (2004) 1953–1964.

[9] R. Romero-Mendez, M. Sen, K. T. Yang, R. McClain, Effect of fin spacing on convection in a plate fin and tube heat exchanger, International Journal of Heat and Mass Transfer 43, (2000) 39-51.

[10] P. Wais, Fin-tube heat exchanger performance for different louver angles, Zeszyty Naukowe Politechniki Rzeszowskiej Mechanika 86, (2014) 115-122.

[11] P. Wais, Influence of fin thickness and winglet orientation on mass and thermal efficiency of cross-flow heat exchanger, Applied Thermal Engineering 102, (2016) 184-195.

[12] A. Erek, B. Ozerdem, L. Bilir, Z. Ilken, Effect of geometrical parameters on heat transfer and pressure drop characteristics of plate fin and tube heat exchangers. Applied Thermal Engineering 25, (2005) 2421–2431.

[13] S. Y. Yoo, H. K. Kwonb, J. H. Kima, A study on heat transfer characteristics for staggered tube banks in cross-flow. Journal of Mechanical Science and Technology 21, (2007) 505- 512.

[14] D. Taler, Methods for obtaining heat transfer correlations for plate finned heat exchangers using experimental and CFD simulated data, Archives of Thermodynamics 25, (2004) 31 54.

[15] D. Taler, P. Ocłoń, Determination of heat transfer formulas for gas flow in fin-and-tube heat exchanger with oval tubes using CFD simulations, Chemical Engineering and Processing 83, (2014) 1–11.

[16] D. Taler, P. Ocłoń, Thermal contact resistance in plate fin-and-tube heat exchangers, determined by experimental data and CFD simulations, International Journal of Thermal Sciences 84, (2014) 309–322.

[17] P. Ocłoń, S. Łopata, M. Nowak, A. C. Benim, Numerical study on the effect of inner tube fouling on the thermal performance of high temperature fin-and-tube heat exchanger, Progress in Computational Fluid Dynamics, An International Journal, 5, (2015) 290–306.

[18] P. Wais, Fin-tube heat exchanger optimization, in: J. Mitrovic, Heat Exchangers – Basics design applications, In-Tech Rijeka, (2012) 343-366.

[19] A. Kraus, A. Aziz, J. Welty, Extended surface heat transfer, A Willey Inter science Publication, 2001.

[20] F. C. McQuiston, D. R. Tree, Optimum space envelopes of the finned tube heat transfer surface, ASHRAE Transactions, Vol. 78, Part 2, (1972) 144-152.

[21] G. H. Hewitt, G. L. Shires, T. R. Bott, Process Heat Transfer, CRC Press, 1994.

[22] R. W. Serth, Process heat transfer: principles and applications, Elsevier USA, 2007.

[23] T. Kuppan, Heat exchanger design handbook, Marcel Dekker USA, 2000.

[24] O. James, J. O. Maloney, Perry's chemical engineers' handbook. Mc Graw-Hill, USA,2008.